Statistical Simulation of Shift Force for a Manual Transmission

Joohyung Kim
Engineer, Samaung Data System,
Maetan-dong, Paldal-gu, Suwon 443-370, Korea
Sangjoon Park
Graduate Student, School of Mechanical Engineering, Sungkyunkwan University,
Chunchun-dong, Jangan-gu, Suwon 440-746, Korea
Hanlim Song
Assistant Professor, Dept. of Computer Applied Mechanical Engineering,
Ansan College of Technology, Choji-dong, Ansan 425-792, Korea
Chaehong Lim
Senior Research Engineer, Manual Transmission Engineering Team,
Hyundai Motor Company, Hwaseong-gun, Gyeonggi-do 445-855, Korea
Hyunsoo Kim*
Professor, School of Mechanical Engineering, Sungkyunkwan University,
Chunchun-dong, Jangan-gu, Suwon 440-746, Korea

Statistical simulation approaches are proposed to evaluate the shift feeling for a manual transmission. First, shift force simulator for the manual transmission is developed by considering the dynamic models of the external and internal linkage, synchronizer, and drivetrain. It is found that the shift force by the simulator shows a good correlation with the test results. Using the simulator, two kinds of statistical simulation approaches are proposed and the objective parameters that can be used to evaluate the shift feeling quantitatively are obtained. It is expected that the shift force simulator with the statistical approaches, developed in this study can be used as a useful design tool to evaluate the shift feeling in the initial design stage.

Key Words : Manual Transmission, Shift Feeling, Probability

1. Introduction

The shift feeling that a driver experiences during the shifting is one of the important factors influencing the evaluation of controllability and operational comfort in the manual transmissions. The importance of shift quality of the manual transmissions has increased significantly over the past few years as the refinement of other vehicle systems has increased.

The shift feeling has been evaluated traditionally in subjective manner by the experienced test driver. In evaluating the shift feeling, the driver judges the evaluation point from many parameters such as easiness of the shift operation, existence of the harshness, clash and etc. If the accurate shift effort, i.e., shift force transmitted to the driver's hand can be predicted, the shift feeling can be evaluated quantitatively in objective manner. However, since the shift feeling is produced by the dynamic interaction between the linkage, shift fork, synchronizer and the drivetrain, it is difficult to figure out the mechanism of these phenomena by experimental approaches, and virtually impossible at concept design stage. To

* Corresponding Author,
E-mail : hskim@me.skku.ac.kr
TEL : +82-31-290-7438; **FAX** : +82-31-290-5849
Professor, School of Mechanical Engineering, Sungkyunkwan University, Chunchun-dong, Jangan-gu, Suwon 440-746, Korea. (Manuscript **Received** September 5, 2003; **Revised** November 27, 2003)

overcome these difficulties, it is required to evaluate the shift feeling by a simulator constructed based on the dynamic models of the manual transmission.

A few studies have been reported on the dynamic modelling of the shift process for the manual transmission. Goto et al.(1998) obtained a simple simulation model for a synchronizing system including the shift control system from the lever to the fork. Analytical model of the synchronizer components was proposed by Hoshino (1998) using ADAMS. In their work, the synchronizing step is divided into six steps such as movement of the sleeve, detent, index, balk, mesh of the sleeve and the outer ring, the mesh of the sleeve and the clutch gear. However, the shift force transmitted to the driver's hand could not be estimated since the dynamic model of the linkage system as well as the drivetrain was not included. Kelly and Kent (2000) developed a gearshift quality dynamic models including the linkage, transmission, driveline and the synchronizer using MATLAB Simulink. The model takes each of the degrees of freedom, and solves for the acceleration of each component either axially or rotationally. Synchronizing motion was analyzed by Shinbata and Nakamura (1991) to investigate the nibble mechanism. They quantified the effect of design parameters on the nibble using experimental results, and a dynamic model covering the sleeve and gear without consideration of the linkage system.

In this paper, a shift force simulator for a manual transmission is developed. Dynamic models of the entire system including the external and internal linkage system, the synchronizer and the drivetrain are obtained. Simulation results are compared with the experimental results from the bench test to validate the dynamic models of the simulator. In addition, statistical approaches are proposed to estimate the shift feeling by considering the variation of the design parameters.

2. Dynamic Model of Manual Transmission

In Fig. 1, a schematic diagram of the shift mechanism from the shift lever to the synchronizer of the manual transmission, investigated in this study, is shown. When the driver pushes or pulls the lever, the displacement of the lever is transmitted to the rubber bushing through the cable. The linear motion of the rubber bushing is transformed into the rotational motion of the shift arm. The rotational motion of the shift arm is in turn transformed into the linear motion of the control shaft, and the shift fork that is attached to the control shaft pushes or pulls the sleeve of the synchronizer, where synchronization occurs. A weight is attached at the end of the shift arm to increase the inertial effect of the linkage system.

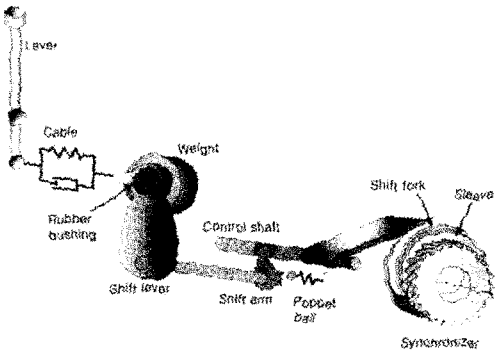

Fig. 1 Schematic diagram of linkage system

2.1 Linkage system

The linkage system consists of the external and the internal system. The external system includes shift lever, cables and rubber bushing. These are modelled as a spring-mass-damper system. In order to determine the stiffness of each element, experiments were performed. The cable stiffness was measured for a layout installed in an assembly. For a given input displacement, the reaction force was obtained. In addition, a gap displacement between the cable core and the outer coat covering the cable core, was measured. It is noted from the experiment that the gap displacement increases with the input displacement while the reaction force is small, but remains almost constant for a relatively large reaction force. This means that, when the lever displacement is small, the input displacement is absorbed to fill the

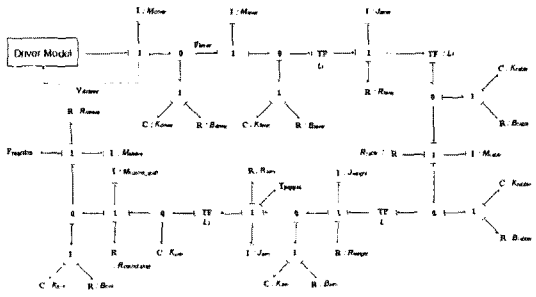

Fig. 2 Bondgraph model of linkage system

gap between the cable core and the outer coat. Once the gap is completely diminished, a linear relationship between the input displacement and the reaction force can be obtained. As for the rubber bushing, a force-displacement relationship was obtained by experiment. The internal linkage mechanism includes poppet ball, control shaft, shift fork and sleeve. The masses, inertias, friction, damping, stiffness and backlash present in the system are modelled. The poppet ball is used to provide a moderate shift feeling to the driver by generating a negative torque when the shift arm rotates over a given range.

In Fig. 2, a Bondgraph model for the entire linkage system is shown (Karnopp, 2000). From the Bondgraph model, state equations of the linkage system can be derived. State equations of the lever velocity, V_{lever}, and the sleeve velocity, V_{sleeve}, are obtained as

$$M_{lever}\dot{V}_{lever}=F_{lever}-[K_{lever}X_{lever}+B_{lever}(V_{lever}-L_f\omega_{lever})] \quad (1)$$

$$M_{sleeve}\dot{V}_{sleeve}=K_{fork}X_{fork}+B_{fork}(V_{control.shaft}-V_{sleeve})-B_{sleeve}V_{sleeve}-F_{reaction} \quad (2)$$

where M_{lever} is the lever mass, F_{lever} is the driver's input lever force, K_{lever} is the lever stiffness, X_{lever} is the relative displacement of the lever, B_{lever} is the lever damping coefficient, L_f is the length from the hand ball to the rotational center of the lever, ω_{lever} is the lever angular velocity, M_{sleeve} is the sleeve mass, K_{fork} is the fork stiffness, X_{fork} is the relative displacement of the fork, B_{fork} is the fork damping coefficient, $V_{control.shaft}$ is the velocity of control shaft, B_{sleeve} is the sleeve damping coefficient and $F_{reaction}$ is the reaction force applied to the sleeve.

2.2 Driver model

In Eq. (1), the shift lever force, F_{lever}, is applied as an input to the linkage system. In the simulator, the shift force transmitted to the driver's hand needs to be calculated as a reaction force by the transmission, which seems to be impossible because no dynamic system can generate effort (force) when the effort is given to the system. In other words, in order to obtain the shift force, the shift lever velocity should be given as the input. In this study, a driver model is introduced to describe the relationship between the driver's intention and the shift lever input force, F_{lever}. The driver's intention can be represented as a velocity of the shift lever motion. Therefore, in the driver model, the shift force can be obtained as the output from the system for the given velocity input.

The target lever velocity can be obtained from the average value of the test results. A proportional, integral, and derivative (PID) controller is used to describe the driver's behaviour. The driver generates the shift lever force corresponding to the reaction force from the linkage system. The driver's arm and hand are modelled as a damped spring-mass system.

2.3 Synchronizer

The synchronizer is an integral element that generates the friction force to reduce the synchronized side speed at upshift or to increase the synchronized side speed at downshift, and changes the power flow. Figure 3 shows a double cone synchronizer used in this study. The double cone synchronizer consists of the sleeve, gear, synchro cone, hub, outer ring and inner ring. In this study, the synchronizing motion is modelled as seven steps as shown in Fig. 4. Each step is determined depending on the relative position of the sleeve to the ring spring, outer ring, and engagement gear as follows:

Step 1 : Sleeve moves from the neutral position until the sleeve contacts the outer ring.

Step 2 : Sleeve and outer ring are in contact.

Step 3 : Outer ring or sleeve is indexed.

Step 4 : Sleeve moves passing the outer ring to

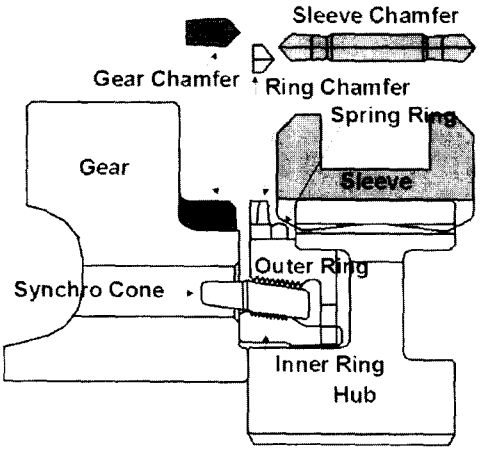

Fig. 3 Synchronizer

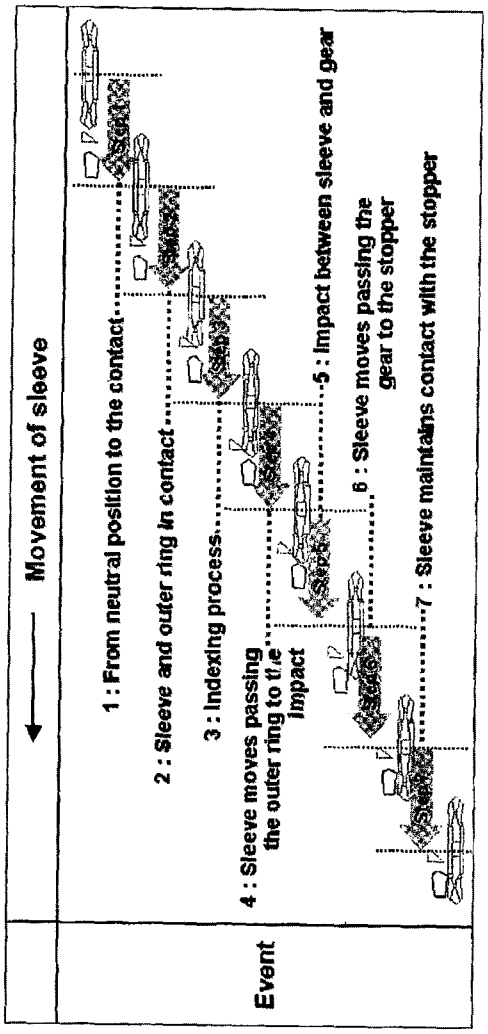

Fig. 4 Synchronizing procedure

the impact point.

Step 5 : Impact between the sleeve and gear.

Step 6 : Sleeve moves past the gear to the stopper.

Step 7 : Sleeve maintains contact with the stopper.

At each step, the shift force transmitted to the driver's hand is determined by the sleeve reaction force. For instance, in step 2, the sleeve reaction force, $F_{reaction}$, can be obtained as

$$F_{reaction}=F_{sleeve.fric}+F_{spr.fric}+F_{spr.axial}+F_{axial} \quad (3)$$

where $F_{sleeve.fric}$ is the sleeve friction, $F_{spr.fric}$ is the spring friction, $F_{spr.axial}$ is the ring spring reaction force in the axial direction. Parameters $F_{spr.fric}$ and $F_{spr.axial}$ can be obtained as the axial component of the friction and the ring spring reaction force. The axial force, F_{axial}, can be obtained from the axial force applied to the ring chamfer, which is explained below.

2.4 Chamfer to chamfer contact model

The contact model is required to calculate the reaction force generated at the contact surface between the sleeve chamfer and the outer ring chamfer. In this study, a spring damper model is used to describe the contact mechanism. The reaction force at the contact surface can be calculated from the deflection between the contact surface, which is determined when the displacements of both contact sides are given. The displacement of the sleeve can be obtained by integrating the velocity of the sleeve, which is determined from the dynamic model of the linkage system. The spring constant for the contact model was obtained from finite-element analysis using ABAQUS. From the contact model, the axial reaction force, F_{axial}, is determined as

$$F_{axial}=K_{contact}\Delta x_{sleeve}+B_{contact}V_{sleeve} \quad (4)$$

where $K_{contact}$ is the contact spring stiffness, Δx_{sleeve} is the deflection at the contact surface and $B_{contact}$ is the damping coefficient. The axial force, F_{axial}, acting on the outer ring chamfer generates the index torque and the cone torque. From a force equilibrium at the contact state in

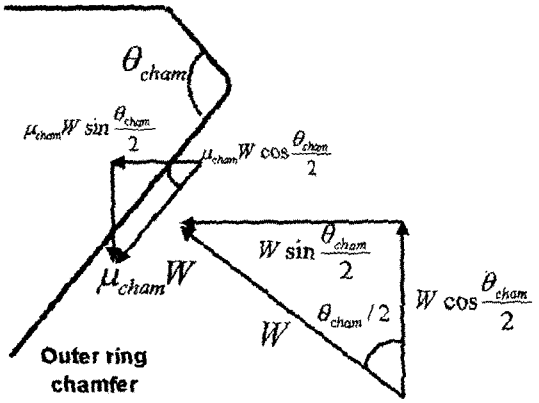

Fig. 5 Forces acting on outer ring chamfer

Fig. 5, the tangential force $F_{ring.tangent}$ to generate the index torque are obtained.

$$F_{ring.tangent} = W \cos\frac{\theta_{cham}}{2} - \mu_{ring.cham} W \sin\frac{\theta_{cham}}{2} \quad (5)$$

$$F_{axial} = W \sin\frac{\theta_{cham}}{2} + \mu_{ring.cham} W \cos\frac{\theta_{cham}}{2} \quad (6)$$

where W is the normal force acting on the sleeve chamfer, θ_{cham} is the angle of the outer ring chamfer, $\mu_{ring.cham}$ is the friction coefficient between the outer ring and sleeve chamfer. From equation (5), (6), $F_{ring.tangent}$ is represented by F_{axial} as

$$F_{ring.tangent} = F_{axial}\left\{\frac{\cos\frac{\theta_{cham}}{2} - \mu_{ring.cham}\sin\frac{\theta_{cham}}{2}}{\sin\frac{\theta_{cham}}{2} + \mu_{ring.cham}\cos\frac{\theta_{cham}}{2}}\right\} \quad (7)$$

The axial force, F_{axial}, and the ring spring force, $F_{spr.axial}$, are used to generate the cone torque. The cone torque, T_{cone}, can be obtained from Fig. 6 as

$$T_{cone} = \frac{\mu_{cone}}{\sin\theta_{cone}} R_{cone}(F_{axial} + F_{spr,axial}) \quad (8)$$

where μ_{cone} is the friction coefficient of cone, θ_{cone} is the angle of cone and R_{cone} is the mean radius of synchro cone.

2.5 Drivetrain

Figure 7 shows a drivetrain model of the manual transmission used in this study. The drivetrain consists of the input and output shaft, 1~5 speed gears, rear gear, 1-2, 3-4 and 5-R synchronizer,

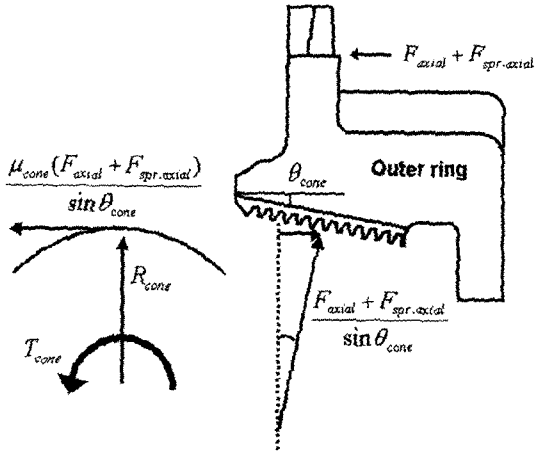

Fig. 6 Cone torque

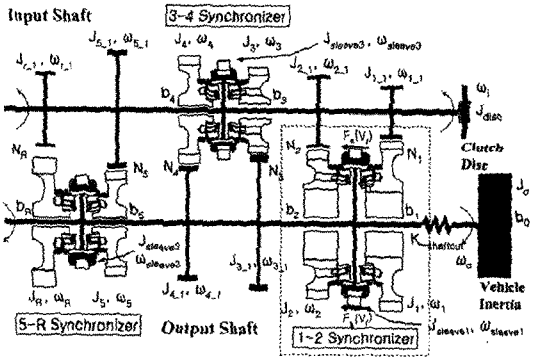

Fig. 7 Drivetrain model

clutch disc and the inertias. In Fig. 7, N is the gear ratio, ω is the speed, J is the inertia, b is the damping coefficient, subscript i is the input shaft, o is the output shaft and number 1~5 denotes the speed range. When the sleeve moves by the driver's lever operation, the friction occurs between the rings and the gear cone, which results in the synchronization. During the synchronization, this friction affects the rotational speed response of the input and the output shaft.

3. Simulation Results and Discussion

In Fig. 8, simulation results for 1-2 upshift are shown. System parameters used in the simulation are shown in Table 1. In the simulation, the target velocity of the driver model was used as $V_{driver}=1$ m/sec, which was obtained as the

Table 1 Parameters used in simulation

Parameter	Value
1st stage gear ratio	3.636
2nd stage gear ratio	2.056
3rd stage gear ratio	1.296
4th stage gear ratio	0.943
5th stage gear ratio	0.756
Mass of lever, M_{lever}	0.4435 kg
Stiffness of popet ball spring, K_{ball}	2381 N/m
Stiffness of lever, K_{lever}	47180 N/m
Mass of sleeve, M_{sleeve}	0.3 kg
Stiffness of fork, K_{fork}	800000 N/m
Friction coefficient between outer ring and sleeve chamber, $\mu_{ring.cham}$	0.1
Friction coefficient of cone, μ_{cone}	0.09
Mean radius of double cone for 1-2 upshift, R_{cone}	72.45 mm

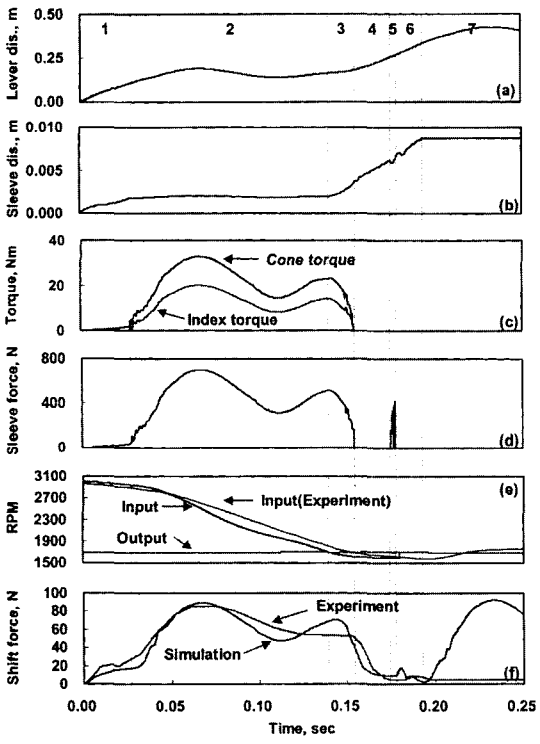

Fig. 8 Simulation and experimental results for 1-2 upshift

average velocity of the shift lever from the bench tests. The time response of the shift lever displacement (a), the sleeve displacement (b), the index and cone torque (c), the sleeve force (d), the input and output speed (e) and shift force (f) are plotted. In addition, experimental results of the input speed and the shift force are compared with the simulation results. The simulation results are divided into seven steps as described in the text. In step 1, as the lever displacement increases, the sleeve moves forward, clearing the gaps between the sleeve and the outer ring. In this step, a small cone torque (c) is generated by the ring spring reaction force. The shift force (f) in this region is represented as a summation of the ring spring force and the poppet ball spring force, which occurs in the opposite direction of the shift lever motion. In step 2, the sleeve chamfer maintains contact with the outer ring chamfer. Therefore, the sleeve displacement (b) remains almost constant. In this step, the driver pushes the shift lever (a) to generate the cone torque (c) that is required to reduce the synchronized side (input) speed for the synchronization. Correspondingly, the input speed (e) decreases and a large shift force (f) is transmitted to the driver. As shown on the input speed response (e), most of the synchronization process is accomplished in step 2. Step 3 is the indexing region where the outer ring chamfers are aligned for the sleeve chamfers to pass through the outer ring chamfers. As the outer ring (gear) speed becomes lower than the output shaft speed (e), the outer ring rotates relative to the sleeve and the sleeve moves forward (b). Therefore, the sleeve force decreases and shows zero value when the outer ring is ready to allow the sleeve to pass between the outer ring chamfers. In step 4, the sleeve moves past the outer ring until it impacts the gear. Since no reaction force is applied to the sleeve (d) while the sleeve is moving, no cone torque (c) is generated. However, the shift force decreases slowly owing to the dynamic characteristics of the linkage system. Step 5 is the impact region between the sleeve and the gear. During step 2 and 3, the linkage mechanism has been compressed, storing the energy in the system. Since the sleeve is released at the end of step 3 by the stored energy, the sleeve impacts the gear in step 5 which results in a spike

in the sleeve force (d). The oscillation of the sleeve force in the impact region means that the impact occurs several times in a short period. However, the shift force (f) shows a relatively small second load peak in spite of the spike in the sleeve force owing to the linkage system dynamics. In step 6, the sleeve chamfer moves forward past the gear chamfers until the sleeve contacts the stopper. The shift process is basically completed in step 6. Step 7 is the region where the driver operates the shift lever after the shift is finished. The large shift force (f) in step 7 is due to the after-motion of the shift lever (a). The shift force in step 7 does not contribute any effect on the shift feeling that the driver experiences. In this study, the dynamic modelling of the synchronized side rotational motion is performed until the sleeve begins to align with the gear, since it can be assumed that the synchronized side (input side) speed is equal to the output speed after the alignment. The discontinuous point in the input speed is due to this assumption. In reality, a speed difference may occur owing to the clearance between the gear and the sleeve. However, the shift force is not affected any more by the relative motion of the sleeve to the gear since no force is exerted to the sleeve except the friction (d) after the alignment between the sleeve and the gear. The shift force (f) after the alignment is due to the dynamic response of the linkage system. Simulation results of the input speed (e) and the shift force (f) are compared with those obtained by the experiments. It can be seen that the simulation results are in good agreement with the experiments.

4. Statistical Simulation of Shift Feeling

The simulation results of the shift feeling in Fig. 8 are obtained using the fixed parameters. However, in actual maneuver of the manual transmission, the input lever velocity can be varied by the driver and the design parameters such as friction coefficient can not be maintained as constant value during the period of the transmission life. Therefore, a statistical approach is inevitable to evaluate the shift feeling that is meaningful to the designer. In this study, two kinds of statistical approaches are proposed to evaluate the shift feeling using the probability density function.

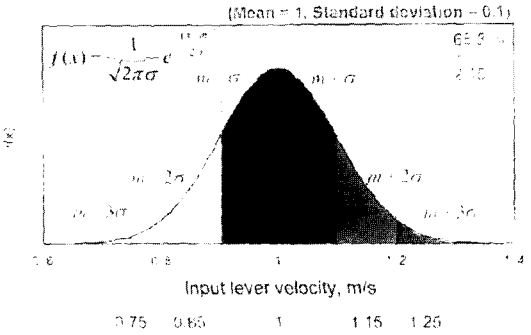

Fig. 9 Probability density function of driver's input lever velocity

4.1 Probability density function

To process the statistical simulation, the probability density function of the design parameters need to be known. In this study, as the design parameters, the driver's input lever velocity, friction coefficient of the synchro cone, damping coefficient of the drivetrain are selected.

Driver's input lever velocity : The mean value of the driver's input lever velocity is obtained as $m=1$ m/sec from the bench test. Assuming that the input lever velocity, V_{lever} has a Gaussian probability distribution and using the mean velocity and the standard deviation, $\sigma=0.1$ m/sec, the probability density function of the input lever velocity is obtained as shown in Fig. 9. It is noted from Fig. 9 that the mean value of V_{lever} is $m=1$ m/sec in the band $m-\sigma$ to $m+\sigma$ and the probability that V_{lever} lies between $m-\sigma$ and $m+\sigma$ is 68.3%.

The probability density function of the synchro cone friction coefficient and the drivetrain damping coefficient can be established in similar manner, using the data from the bench test results.

Impact position of chamfers : When synchronization is carried out, magnitude of the second load peak varies depending on the relative position of the impact between the sleeve chamfer and the gear chamfer. Since the impact position

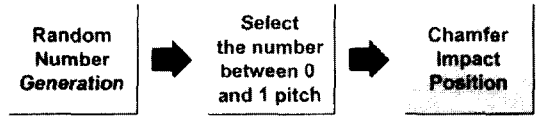

Fig. 10 Random generation of chamfer impact position

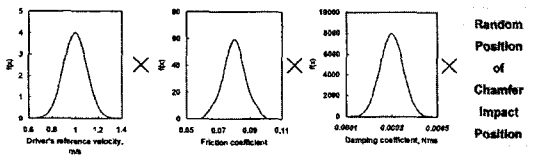

Fig. 11 Simulation procedure for statistical approach (I)

is determined in an arbitrary manner, the randomness of the chamfer impact position is considered as shown in Fig. 10. First, the random number is generated from MATLAB Simulink, and this random number is converted into the pitch position between 0 to $2\pi/z$, where z is the number of the sleeve chamfer teeth.

4.2 Statistical simulation

For the statistical simulation, two kinds of simulation method are proposed.

Statistical approach (I): In Fig. 11, the simulation procedure for the statistical approach (i) is shown. Simulation is performed using the combination of three design parameters and the impact position that is determined randomly. The total number of simulation is 125, which is a product of the five representative values for three variables. This approach is basically same with the Monte Carlo method.

From the statistical approach (I), probability density function of the objective parameters that can be used to evaluate the shift feeling quantitatively, are obtained as shown in Fig. 12. In Fig. 12, probability density function of the selected objective parameters such as time shift integral are shown with the mean and standard deviations.

Statistical approach (II): Statistical approach (II) proposed in this study can be explained as follows; If X_n is the nth input lever velocity which has the probability α_n, Y_m is the m_{th} friction coefficient which has the probability β_m,

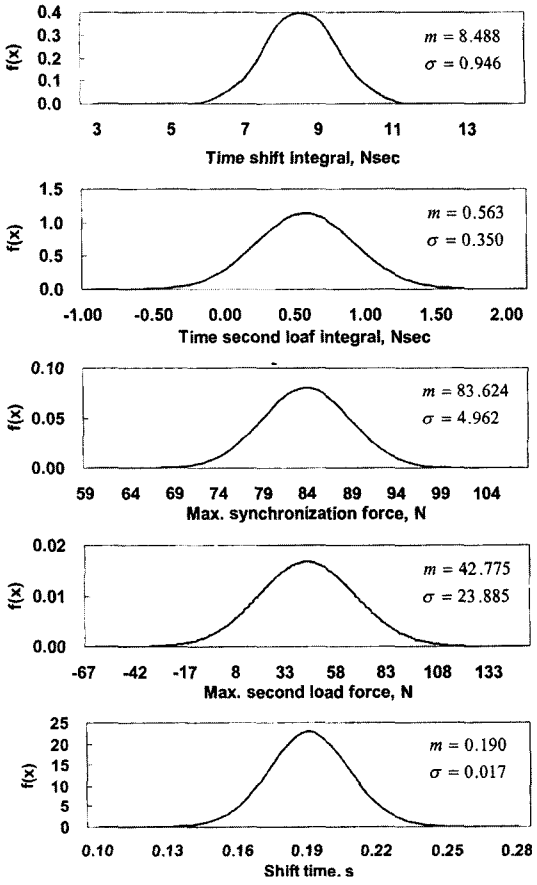

Fig. 12 Probability density function of objective parameters

and z_k is the k_{th} damping coefficient of the drivetrain, that has the probability γ_k, the simulation results of the objective parameter $R_{n,m,k}$ is defined as

$$R_{n,m,k}=\text{simulation result using } X_n,\ Y_m,\ Z_k \quad (9)$$

Therefore, the representative value of the objective parameter R can be obtained by considering the probability as

$$\begin{aligned}\text{Representative value of}\\ \text{R}=&R_{1,1,1}\times\alpha_1\beta_1\gamma_1+R_{1,1,2}\times\alpha_1\beta_1\gamma_2+\cdots\\ &+R_{n,m,k-1}\times\alpha_n\beta_m\gamma_{k-1}+R_{n,m,k}\times\alpha_n\beta_m\gamma_k\end{aligned} \quad (10)$$

$$\text{n}=1,\ 2,\ \cdots,\ 5$$

$$\text{m}=1,\ 2,\ \cdots,\ 5$$

$$\text{k}=1,\ 2,\ \cdots,\ 5$$

Table 2 Simulation results of objective parameters for 1-2 upshift

Objective parameter	Approach (I)	Approach (II)
Time shift integral	m=8.488 Nsec	8.274 Nsec
	σ=0.946 Nsec	
Time second load integral	m=0.563 Nsec	0.499 Nsec
	σ=0.350 Nsec	
Max. synchronization force	m=83.624 N	83.089 N
	σ=4.962 N	
Max. second load force	m=42.775 N	41.805 N
	σ=23.885 N	
Shift time	m=0.190 sec	0.186 sec
	σ=0.017 sec	

Objective parameters obtained by the statistical approach (II) are compared with those by the approach (I) in Table 2. It is seen that the objective parameters by the two methods show almost the same values.

4.3 Statistical analysis in time domain

Statistical analysis in time domain provides an insight to the design engineer since the effect of the design parameter on the behavior of the objective parameters can be investigated directly in the time domain. The time domain analysis is performed by varying the one design parameter while using the representative values of the other two parameters, that have the most probability.

In Fig. 13, results of the time domain analysis of the double cone synchronizer for 1-2 upshift are shown. The simulations are performed by varying the driver's input lever velocity while using the most probable representative values of the cone friction coefficient and the damping coefficient. It is noted from the statistical analysis in the time domain that as the input lever velocity increases, the first peak of the shift force increases while the required shift time becomes shorter, which seems quite natural by considering the operation of the manual transmission. However, the second load peak does not depend on the input lever velocity because the second load peak is determined by the relative position between the sleeve and the gear chamfer, which requires the statistical approach mentioned earlier.

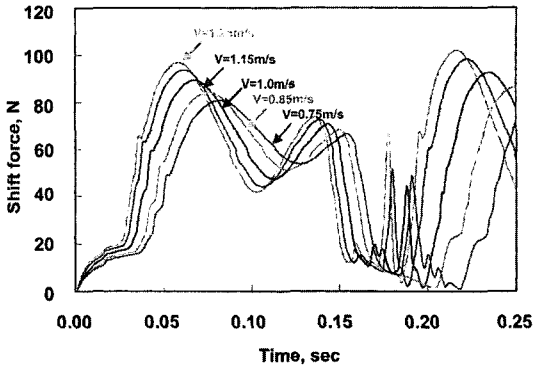

Fig. 13 Statistical analysis in time domain for input lever velocity at 1-2 upshift

5. Conclusions

Statistical simulation approaches are presented to evaluate the shift feeling for a manual transmission. To investigate the shift force, shift force simulator is developed by considering the dynamic models of the external and internal linkage, synchronizer, and drivetrain. The synchronizing motion is modelled as seven steps depending on the relative displacement of the sleeve to the ring spring, outer ring and engagement gear. It is found that the shift force by the simulator shows a good correlation with the test results. Using the simulator, two statistical simulation approaches are proposed. From the statistical simulations, the objective parameters that can be used to evaluate the shift feeling quantitatively, are obtained. It is expected that the shift force simulator with the statistical approaches developed in this study can be used as a useful design tool to evaluate the shift feeling in the initial design stage.

References

Goto, Y., Yagi, Y., Morimoto, Y. and Kawasaki, M., 1998, "Shift Feel in Manual Transmissions-An Analysis of Unsmooth Shifting and Gear Clashing," *JASE Review*, Vol. 9, No. 4, pp. 52~55.

Hoshino, H., 1998, "Simulation on Synchronization Mechanism of Transmission Gearbox,"

International ADAMS User Conference.

Karnopp, D. C., Margolis, D. L. and Rosenberg, R. C., 2000, *System Dynamics*, John Willey & Sons, Inc.

Kelly, D. and Kent, C., 2000, "Gear Shift Quality Improvement in Manual Transmission Using Dynamic Modelling," *FISITA World Automotive Congress.*

Shinbata, K. and Nakamura, N., 1991, "Achievement of Theoretical Quantitative Evaluation Method and Effective Countermeasures for Manual Transmission Nibble," SAE Paper 912524.